

Nanofabrication by current stimulated atomic migration

A. V. Silhanek^{1,*}, J. Lombardo¹, W. Keijers², J. Van de Vondel²

¹ Experimental Physics of Nanostructured Materials, Q-MAT, CESAM, Universite de Liège, B-4000 Sart Tilman, Belgium.

² Laboratory of Solid-State Physics and Magnetism, KU Leuven, Celestijnenlaan 200D, 3001 Leuven, Belgium.

*asilhanek@uliege.be

The displacement of atoms caused by high electric current densities was already identified in the late 1960s as a major problem of narrow Al interconnects in integrated circuits and other electronic devices. The negative perception of this phenomenon, known as electromigration, has progressively changed during the last decades, as the scientific community first understood the physical mechanisms involved in the process and then learnt to master it. Nowadays, controlled electromigration can be regarded as a very promising tool for modifying the physical properties of micro and nanoscale materials with single atom resolution and with a high degree of flexibility. In this work, we adopt this emerging technique to achieve in situ targeted modulation of the materials properties in superconducting devices.

Introduction

Electromigration (EM) is the displacement of ions in a metal resulting from the momentum transfer between conducting electrons and diffusing atoms [1]. Although its discovery can be traced back to more than 100 years ago, it became a major problem only when the extreme conditions necessary for operation of integrated circuits made it apparent in the late 1960s.

In conventional wires such as those used for domestic applications, the current density is limited to about 10^4 A/cm² due to Joule heating. Current densities exceeding this value will produce enough heat to melt the metal wire. In this case, electromigration is not a serious concern. However, in micro and nanoscale circuits, where heat evacuation is more efficient, current densities of 10^6 A/cm² or even higher can circulate without burning the circuit. At these high current densities, electromigration becomes significant and an important cause of failure.

The initial negative perception of this stochastic process has progressively evolved. Nowadays, it can be considered as an emerging technique for specifically targeting local modifications of metallic nanocircuits. More importantly, this is achieved with few atom precision, at low cost, and surpassing the possibilities offered by conventional electron beam lithography. Examples illustrating the benefits of controlling the EM process include the creation of few nanometer gaps between two Au pads [2] with the aim to electrically address single molecules [3], the electrical sculpting of nanowires to obtain atomic point contacts [4], the possibility to achieve metal purification and separation

of atoms in binary alloys due to the mass selectivity of the process, and the cleaning of 2D materials [5].

Some concrete examples of recent applications of controlled electromigration as a nanofabrication tool for modifying the local material properties of superconducting devices, are briefly discussed in the following sections.

In situ tailoring of superconducting Nb junctions via electro-annealing

The investigated samples consist of 50 nm-thick Nb films deposited by electron beam evaporation onto a Si substrate terminated with a 100 nm-thick SiO₂ layer under UHV and subsequently capped with 5 nm of Si for protection. The Nb film is patterned via electron beam lithography in a bow-tie shape (see left panel of Fig.1) so that even a relatively small applied current can have significant impact due to its crowding (i.e. large density) at the narrowest point of the sample (130 nm).

Controlled EM was achieved by applying a software-controlled voltage to the sample. Typical values of current needed to electromigrate our devices are on the order of a few mA to 10 mA. The EM setup is based on a four point probe measurement scheme. This allows us to directly measure the conductivity of a nanostructure by using a current source and a voltmeter. In these experiments, the control feedback algorithm decides to increase or decrease the applied bias trying to keep the variation of conductance dG/dt at the value set by the operator. This process continues until the desired re-

sistance of the constriction is reached. The details of the electromigration software are described in Ref. [6].

By progressively increasing the applied current, we first identify a regime of current densities at the constriction below 10^8 A/cm², at which the superconducting properties of the constriction are slightly improved compared to the lateral banks. Within this regime the superconducting critical temperature (T_c) and critical current (I_c) increase, while the normal state resistance (R_n) decreases, thus transforming the system in a S–S'–S junction with $T_c(S') > T_c(S)$. When the applied current (electro-annealing current) is increased above 10^8 A/cm², a rapid deterioration of the superconducting properties takes place in the constriction, and the system switches to a S–S'–S junction with $T_c(S') < T_c(S)$. In other words, a weak link is formed. Under such circumstances, one expects the critical current to decline and eventually exhibit Fraunhofer-like oscillations as a function of the out-of-plane magnetic field, as shown in the right panel of Fig.1. These oscillations can be regarded as a fingerprint of a superconducting weak link.

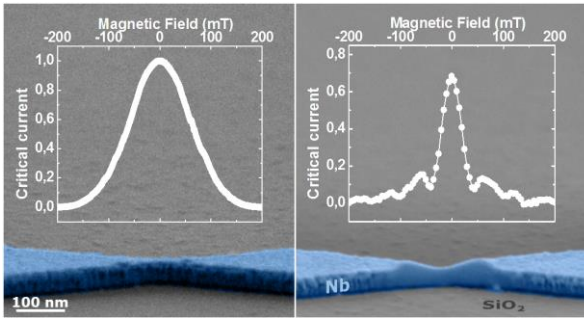


Fig. 1. Tilted angle scanning electron microscopy images of the virgin (left) and after electro-annealing (right) Nb constriction. The insets show the normalized critical current of the device as a function of the external magnetic field. The response of the virgin sample (left panel) is featureless whereas that from the electro-annealed device (right panel) shows a distinct Fraunhofer-like oscillatory dependence.

Nb is a refractory material with relatively small self-diffusion coefficient able to sustain large heating. As a consequence, increasing current triggers other effects before atom migration manifest itself. In order to emphasize this point, we coined this process *electro-annealing*. A high-resolution scanning electron microscopy investigation allowed us to identify an amorphization of the material at the central region of the constriction after applying a large current density [7].

Since during this process a local temperature as high as 970 K can be reached at the constriction, the amorphization may result from the combined effects of high temperature and oxygen diffusion in Nb which is known to become important above 400 K. An additional (additive) effect is the possible contamination of the Nb by the silicon substrate to form Nb₅Si₃ during EM.

Unfortunately, the changes produced by electro-annealing in the Nb constriction described above, are nearly irreversible. However, performing a similar procedure in an Al bridge leads to the creation of voids that can be reversibly healed by simply inverting the direction of the applied current [8].

Geometry control of an Al superconducting quantum interference device by stimulated atom diffusion

It has been shown that the use of controlled electromigration on a pre-indented Al bridge permits to down scale the junction size towards a few atoms [4]. In Ref.[9] we extend this approach by electromigrating two parallel Al constrictions forming a superconducting quantum interferometer device (SQUID) and map the asymmetric reduction of the critical current of the weak links. As a consequence of the critical current reduction, the device suffers less from self-heating thus allowing the phase coherence to persist in the dissipative state.

The initial sample is an aluminium nano-SQUID (thickness $d = 30 \pm 2$ nm), with a central hole area of $0.31 \mu\text{m}^2$ and two constrictions of approximately 50 nm width, as shown in the main panel of Fig. 2. At a temperature $T = 1.5$ K, the resistance of the virgin nano-SQUID in the normal state is $R = 7.99 \pm 0.05 \Omega$. The critical temperature, defined as the onset of the resistance drop, $T_c = 1.32 \pm 0.01$ K, the coherence length at zero temperature is $\xi(0) = 140 \pm 10$ nm, and the resistivity $\rho = 3.9 \pm 0.3 \mu\Omega \text{ cm}$.

After confirmation that the current-phase relationship of the used bow-tie junctions is well described by the Kulik-Omel'yanchuk (KO) model [10], we investigated the quantum interference effects. This phenomenon manifests itself as a distinct oscillation of the critical current of the device as a function of field for temperatures below the superconducting transition temperature (inset in Fig. 2). The data obtained at 300 mK are fitted with an asymmetric SQUID model described in Ref.[11] using the KO current-phase relationship from

which we estimate a total inductance of $L = 8.5 \pm 1.0$ pH, mainly dominated by the kinetic inductance.

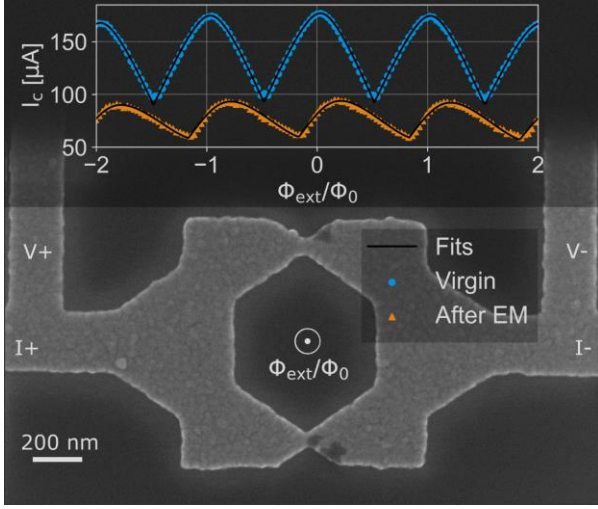


Figure 2. Main panel: scanning electron microscopy image of the thin film Al nano-SQUID after electromigration. The inset shows the dependence of the critical current of the device as a function of the magnetic flux piercing the central hole for the virgin sample (blue curve) and the electromigrated sample (orange curve). The solid black curves represent fitting of the data with the asymmetric SQUID model [11].

Let us now explore the possibility to modify the properties of the nano-SQUID using controlled electromigration. In order to map the evolution of its superconducting properties during EM, the process was halted after a targeted reduction of conductance was obtained, then the nano-SQUID was characterized, and afterwards EM was resumed. This process was repeated several times until a gap was generated at the constriction. The EM was performed inside the cryostat at a temperature of 4.2 K.

An example of the critical current oscillations after EM is shown in the inset of Fig.2 where it is possible to observe a decrease in the oscillation modulation amplitude, a shift of the maximum critical current in magnetic field and an increase in skewness. The origin of these features can be accounted for by an increase in weak link asymmetry. Asymmetry of the junctions becomes advantageous in certain applications. Introducing asymmetry shifts the “blind spots” [12] found at magnetic fields where the I_c interference pattern reaches an extremum. This enables, for example, zero-field sensitivity without any additional sophisticated electronics. Furthermore, sufficient removal of the material

from the weak link reduces its critical current, resulting in the absence of potentially detrimental heating effects. As a result of negligible heating, the SQUID’s dissipative state becomes accessible.

Discussion

It is important to note that in the above discussed examples, EM takes place in the normal state. Indeed, in principle, superconducting nanocircuits are not concerned by atomic migration problems chiefly because in the non-dissipative superconducting state, there is no net momentum transfer between the carriers (Cooper pairs) and the atomic lattice. Furthermore, in low critical temperature superconductors such as Al and Nb, the critical current density lies well below the current density needed to start displacing atoms.

Interestingly, this scenario may no longer hold for cuprate superconductors. The reason is twofold; on the one hand, the atomic diffusion barrier can be relatively weak for certain atoms like oxygen in $YBa_2Cu_3O_{7-d}$, consequently reducing the electromigration current density. On the other hand, these compounds exhibit high superconducting critical current densities. Under these circumstances, when the dissipative state is accessed by applying a current density exceeding the critical value, the component of the current carried by the quasiparticles can surpass the electromigration current density and produce irreversible damage to the material even at local temperatures substantially lower than the melting point of the compound. We have recently addressed this phenomenon in Ref.[13].

This work was done in collaboration with X.D.A. Baumans, V. Zharinov, R.B.G. Kramer, R. Pangotra, Ž. L. Jelić, M.V. Milošević, V.V. Moshchalkov, J.E. Scheerder, and J.P. Nacenta. The research was supported by the Flemish Science Foundation (FWO-VI, Project No. G.0B53.15), the KU Leuven Internal Funds Project No. CREA/14/011, the COST action NanoCoHybri (CA16218), and the F.R.S.-FNRS (PDR T.0106.16). J. Lombardo acknowledges support from F. R. S.- FNRS (FRIA Research Fellowship). The work of A.V.S. is partially supported by the grant CDR J.0151.19 of the F.R.S.-FNRS. The authors thank the ULg Microscopy facility CAREM for part of the SEM investigations. The LANEf framework (ANR-10-LABX-51-01) and the Nanoscience Foundation are

acknowledged for their support with mutualized infrastructure.

References

1. J. R. Loyd // *Semicond. Sci. Technol.*, V. 12, 1177 (1997).
2. M. F. Lambert *et al.* // *Nanotechnology*, V. 14, 772 (2003).
3. J. Park *et al.* // *Nature*, V. 417, 722 (2002).
4. X. D. A. Baumans *et al.* // *Nat. Commun.*, V. 7, 10560 (2016).
5. J. Moser, A. Barreiro, A. Bachtold // *Appl. Phys. Lett.*, V. 91, 163513 (2007).
6. V. S. Zharinov *et al.* // *Rev. Sci. Instrum.*, V. 89, 043904 (2018).
7. J. Lombardo *et al.* // *Nanoscale*, V. 10, 1987 (2018).
8. X. D. A. Baumans *et al.* // *Small*, V. 13, 1700384 (2017).
9. W. Keijers *et al.* // *Nanoscale*, V. 10, 21475 (2018).
10. I. O. Kulik and A. N. Omel'yanchuk // *JETP Lett.* V. 21, 96 (1975).
11. C. D. Tesche and J. Clarke // *J. Low Temp. Phys.*, V. 29, 301 (1977).
12. A. Uri *et al.* // *Nano Lett.*, V. 16, 6910 (2016).
13. X. D. A. Baumans *et al.* // *Appl. Phys. Lett.*, V. 114, 012601 (2019).